4-1-1994

X-rays from Microstructured Targets Heated by Femtosecond Lasers

S. P. Gordon
University of California - Berkeley

Thomas D. Donnelly
Harvey Mudd College

A. Sullivan
University of California - Berkeley

H. Hamster
University of California - Berkeley

R. W. Falcone
University of California - Berkeley

X rays from microstructured targets heated by femtosecond lasers

S. P. Gordon, T. Donnelly, A. Sullivan, H. Hamster, and R. W. Falcone

Department of Physics, University of California, Berkeley, Berkeley, California 94720

Received September 15, 1993

We have demonstrated efficient conversion of ultrashort-pulse laser energy to x rays with energies above 1 keV, using laser-produced plasmas generated on a variety of microstructured surfaces. Lithographically produced grating targets generated 0.1 mJ of kilo-electron-volt x rays, and porous gold and aluminum targets emitted 1 mJ. This represents an improvement of a factor of 100 over flat targets. The K-shell emission spectrum of porous aluminum was composed primarily of heliumlike spectral lines.

Subpicosecond x-ray pulses have applications as short-wavelength flash lamps for photoionization-pumped x-ray lasers[1,2] and as sources for time-resolved x-ray scattering experiments.[3,4] Instrument-limited picosecond bursts of x rays were measured from the near-solid density plasmas by intense ultrashort-pulse lasers focused on solid-metal targets.[5–7] The resulting plasmas cool rapidly as a result of heat conduction into the underlying cold solid and expansion into the vacuum, thereby abruptly quenching x-ray emission.

Unfortunately solid-density plasmas reflect most of the incident laser radiation because of the high refractive index at the target surface. Somewhat increased absorption can be achieved with p-polarized laser light, incident at an angle with respect to the surface normal, because of resonance absorption and vacuum heating[8–11]; however, with flat targets this implies a reduction of the incident laser intensity. Since the conversion efficiency of laser energy to x rays in solid plasmas increases with intensity,[12] normal incidence is desirable. The optimal target should therefore be structured to employ these absorption mechanisms with a normally incident beam.

Enhanced absorption by gratings and porous targets was previously demonstrated at laser intensities as high as 10^{16} W/cm^2.[13] The study described here and related research at Lawrence Livermore National Laboratory[14] extend the study of these interactions to intensities as high as 10^{18} W/cm^2. Our laser system uses a self-mode-locked Ti:Al_2O_3 oscillator that is amplified as described in Ref. 15; it generates pulses with 130-fs duration and 200-mJ energy at 0.8 μm. These pulses were focused at a 10° incidence angle with a 15-cm off-axis parabolic mirror to a 9-μm focal spot on target. X-ray emission above 1 keV was monitored with an x-ray diode (UDT X-UV100) filtered by 25 μm of beryllium. A 0.7-T magnetic deflector was used to avoid spurious signals from hot electrons. Spectra of x rays between 1.45 and 2.1 keV were obtained with a crystal (KAP) spectrometer in a von Hamos configuration.

The first targets employed in our studies were gratings produced by photolithographic techniques. They effectively absorb laser light if the light is polarized perpendicular to the grating grooves. Since the light is p polarized with respect to the walls of the grating, absorption can be significant, even for the steep plasma gradients expected in ultrashort-pulse experiments. Rae and Burnett[11] showed theoretically that a plasma with a surface density gradient 100 times shorter than the laser wavelength is capable of absorbing one half of the energy of an obliquely incident intense laser pulse. Assuming that light propagating in the grating grooves is subject to this absorption on the grating walls, we can estimate the absorption depth δ of the laser in the grooves. The energy loss at the surface may be written as $\partial E/\partial A \approx -0.5E_0/A$, where ∂A is a surface-area element, E_0 is the incident energy, and A is the beam area. For a structure with a volume-to-surface-area ratio (V/SA) that is constant as a function of depth z, $\partial A = (\mathrm{SA/V})\partial \mathrm{V} = (\mathrm{SA/V})A\partial z$. The differential equation for energy loss then becomes $\partial E/\partial z \approx -0.5(\mathrm{SA/V})E_0$. Thus the absorption depth δ is approximately given by 2V/SA.

For a grating, $\mathrm{V/SA} = (l\Lambda d)/(2ld) = \Lambda/2$, where d is the groove depth, l is the length of the exposed area, and Λ is the period; thus $\delta \approx \Lambda$. The absorption depth is therefore expected to be insensitive to target composition and fill factor, which is consistent with the results of previous experiments.[13] However, if the thickness of the walls is small compared with the nominal heat penetration depth during the laser pulse (≥50 nm),[12] such gratings should reach higher temperatures than massive targets, thus further enhancing the emitted x-ray efficiency. The optimal grating target has a small period and thin walls.

X-ray output versus incident laser energy for a 0.6-μm period grating overcoated with 60 nm of aluminum is shown in Fig. 1. For comparison the output from an aluminum-coated glass slide and from a polished silicon wafer is also shown. A 30% larger signal was obtained from the same grating coated with 50 nm of gold and from a 0.7-μm period grating coated with silver. The somewhat enhanced emission of the aluminum-coated slide compared with the

0146-9592/94/070484-03$6.00/0

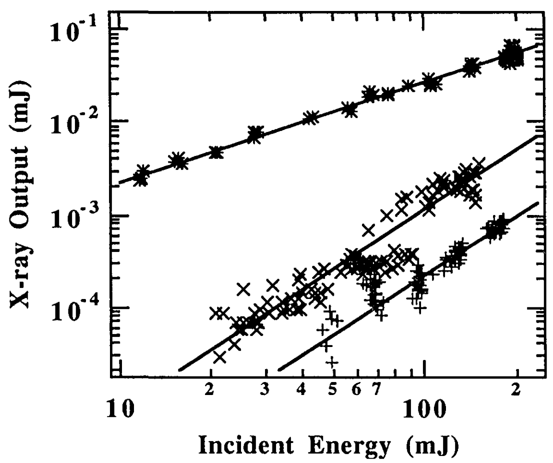

Fig. 1. X-ray emission above 1 keV versus laser energy from an aluminum-coated grating (*), flat aluminum (×), and a silicon wafer (+). The grating data are fit to a power law with an exponent of 1.1 and both solid targets to 2.1.

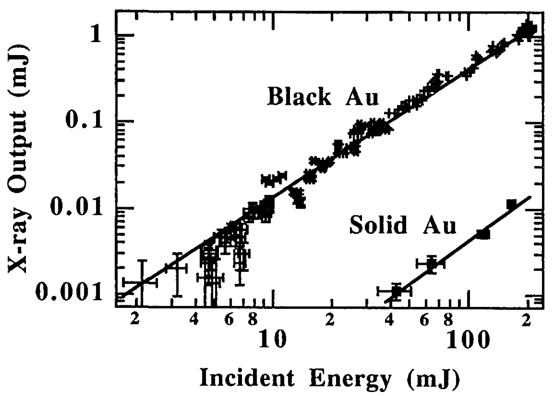

Fig. 2. X-ray emission above 1 keV versus laser energy from porous gold and flat gold. The gold black data are fit to a power law with an exponent of 1.5 and the solid target to 1.7.

silicon wafer can most likely be attributed to a small amount of surface roughness.

Our second type of target is a porous form of metal that appears black. In particular, porous gold, called gold black or gold smoke, absorbs well throughout the visible and into the infrared.[16,17] This material is produced by evaporation of the metal in a few Torr of argon or nitrogen and has an average density 400 times below solid. It is composed of micrometer-sized fractal clusters formed by diffusive growth of 10-nm particles. Theories of infrared absorption by this material at room temperature require detailed knowledge of its fractal structure[18] or at least rudimentary accounting for the proximity and connectedness of neighboring particles.[19–21]

When this material becomes hot as a result of laser absorption, these cluster effects are likewise expected to be important. However, we can estimate the absorption coefficient in the same manner as for the gratings by assuming that absorption is predominantly a surface effect. In this case, V/SA = V_c/NA_p, where V_c is the cluster volume $(4\pi R_c^3/3)$, A_p is the surface area per particle $(4\pi R_p^2)$, and N is the number of particle per cluster. For a fractal, $N = (R_c/R_p)^D$, where R_c is the cluster radius, R_p is the particle radius, and D is the fractal dimension.[18] D may be estimated by use of the average density $\bar{\rho} = \rho_s(R_c/R_p)^{D-3}$, where ρ_s is the solid density. This simple treatment predicts an absorption depth of $\delta \approx R_c^{3-D}/R_p^{2-D}$. Typically $R_c \approx 1$ μm, $R_p \approx 5$ nm, and $D \approx 1.9$, so the absorption depth is expected to be approximately 2 μm. As a result of the long thermal gradient, thermal conduction during the laser pulse is not important. Since a 2-μm absorption depth in porous gold contains as many atoms as a 5-nm depth of solid, the heated mass of material in the porous target would be ten times smaller than that in the flat target and could therefore become as much as ten times hotter.

Gold black emitted >1 mJ of x rays above 1 keV with 200 mJ of energy on target. No variation of x-ray intensity was detected with the diode placed at various angles within $\pm\pi/4$ rad from the normal. In comparison, flat gold was 100 times less efficient. Figure 2 shows the measured output as a function of incident laser energy for porous and flat-gold targets. A target characterized by a gradually increasing gold-black depth was used to determine the absorption depth of this material. The x-ray output of this target reached 90% of its asymptotic value at a depth of 1–2 μm. This measurement approximates the expected depth, as calculated above.

When a porous target was prepulsed with amplified spontaneous emission from the laser amplifiers with sufficient energy to damage the structure before the arrival of the main energy pulse, the x-ray output was reduced by a factor of 20. Thus the actual microscopic structure of these targets, and not merely the low average atom density, is important to their effectiveness. Measurement of the x rays transmitted through progressively higher atomic-number filters revealed extremely nonthermal emission; emission between 2 and 10 keV was characterized by a 700-eV temperature, and emission between 10 and 30 keV was characterized by a 3-keV temperature. The emission from solid gold was similarly nonthermal, with a 1-keV fit between 2 and 10 keV.

It is possible to produce other porous materials with the same evaporation technique used for gold. Since K-shell spectra from a variety of aluminum plasmas have been published,[6,7,22] we examined porous aluminum that had a density 1.5% that of solid. This material generated x rays >1 kV almost as efficiently as the gold and was likewise shown to be much more efficient than a flat-aluminum target. With 150 mJ of energy on target, porous aluminum emitted > 0.5 mJ, compared with 3 μJ from solid aluminum. A thin porous-aluminum target with a depth gradient was employed to determine the approximate absorption depth; in this case the measured depth was 15–20 μm. The absorption-depth theory described above does not seem to explain this order-of-magnitude increase of δ over gold black.

We modeled the temperature and density of aluminum black as a function of time, assuming an initial heated depth of 20 μm and ionization to the heliumlike stage. We used flux-limited thermal dif-

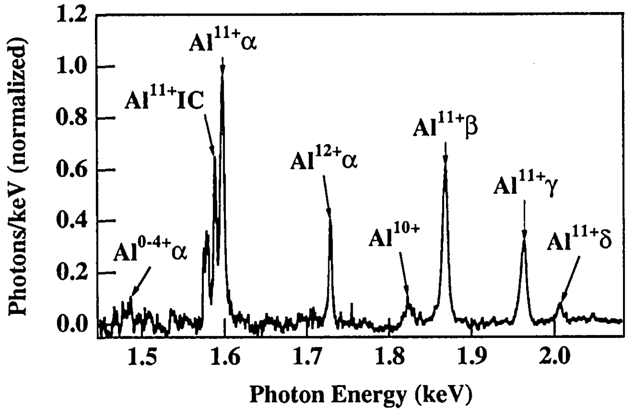

Fig. 3. K-shell spectrum of porous aluminum taken at 10^{18} W/cm^2.

fusion at the average density of the structure and isentropic expansion of the particles following the laser pulse. Radiation cooling was found to be minimal. With the assumption that the average density of the structure, the cluster radius, and the fractal dimension remain constant, expansion into the voids implies cooling according to

$$T \propto \rho_p{}^{\gamma-1} \propto R_p{}^{0.67(D-3)},$$

where T is the temperature, ρ_p is the particle density (initially solid density), and $\gamma = 5/3$ is the specific-heat ratio. This calculation predicts a peak temperature during the laser pulse of 4 keV, with rapid cooling in the following picosecond to 500 eV. The local electron density at this time has dropped to $4 \times 10^{22}/\text{cm}^3$—an order of magnitude less than solid density. Cooling and expansion then continue at a slower pace, reaching 200 eV and $1.5 \times 10^{22}/\text{cm}^3$ after 4 ps.

A spectrum of porous-aluminum emission is shown in Fig. 3. The dominant emission lines are the heliumlike (Al^{11+}) series and the hydrogenlike (Al^{12+}) $2p-1s$ line. The presence of the intercombination line indicates below-solid densities. Comparison of the relative intensities and Stark broadening of the $1snp-1s^2$ ($n = 4-7$) lines with those predicted by the RATION plasma code indicates a density near 3×10^{22} electrons/cm^3 and a temperature of 300 eV. The $K\alpha$ line from unionized aluminum is conspicuously absent from these spectra; this line is usually present in solid-density plasmas because hot electrons excite the underlying cold material. We looked for this interaction in a separate experiment, using a target composed of thin gold black deposited onto solid aluminum; again, the $K\alpha$ line was not present. This implies that forward-directed superthermal electrons are not generated in the porous material.

In summary, we have demonstrated enhanced x-ray emission by gratings and porous targets to incident laser intensities of as high as 10^{18} W/cm^2. We measured 1 mJ of x rays above 1 keV emitted in a broad bandwidth from porous gold and 0.5 mJ in K-shell lines from porous aluminum.

This study was supported by the U.S. Air Force Office of Scientific Research and through a collaboration with Lawrence Livermore National Laboratory under contract W-7405-ENG-48. We thank R. L. Sheperd and D. F. Price for useful conversations, R. W. Lee for the use of his RATION plasma code, M. D. Perry and S. R. J. Brueck for the production of grating targets, and D. W. Phillion for providing software to analyze the x-ray film data.

References

1. H. C. Kapteyn, Appl. Opt. **31,** 4931 (1992).
2. D. C. Eder, G. L. Strobel, R. A. London, M. D. Rosen, R. W. Falcone, and S. P. Gordon, in *Short Wavelength V: Physics with Intense Laser Pulses,* M. D. Perry and P. B. Corkum, eds., Vol. 17 of OSA Proceedings Series (Optical Society of America, Washington, D.C., 1993), p. 220.
3. J. Z. Tischler, B. C. Larson, and D. M. Mills, Appl. Phys. Lett. **52,** 1785 (1988).
4. K. Murakami, H. C. Gerritsen, H. van Brug, F. Bijkerk, F. W. Saris, and M. J. van der Wiel, Phys. Rev. Lett. **56,** 655 (1986).
5. M. M. Murnane, H. C. Kapteyn, M. D. Rosen, and R. W. Falcone, Science **251,** 531 (1991).
6. P. Audebert, J. P. Geindre, J. C. Gauthier, A. Mysyrowicz, J. P. Chambaret, and A. Antonetti, Europhys. Lett. **19,** 189 (1992).
7. J. C. Kieffer, M. Chaker, J. P. Matte, H. Pepin, C. Y. Cote, Y. Beaudoin, T. W. Johnston, C. Y. Chien, S. Coe, G. Mourou, and O. Peyrusse, Phys. Fluids B **5,** 2676 (1993).
8. F. Brunel, Phys. Rev. Lett. **59,** 52 (1987).
9. P. Gibbon and A. R. Bell, Phys. Rev. Lett. **68,** 1535 (1992).
10. U. Teubner, J. Bergmann, B. van Wonterghem, F. P. Schafer, and R. Sauerbrey, Phys. Rev. Lett. **70,** 794 (1993).
11. S. C. Rae and K. Burnett, Phys. Rev. A **44,** 3835 (1991).
12. M. D. Rosen, Proc. Soc. Photo-Opt. Instrum. Eng. **1229,** 160 (1990).
13. M. M. Murnane, H. C. Kapteyn, S. P. Gordon, J. Bokor, E. N. Glytsis, and R. W. Falcone, Appl. Phys. Lett. **62,** 1068 (1993).
14. R. Shepherd, D. Price, W. White, A. Osterheld, R. Walling, W. Goldstein, R. Stewart, and S. P. Gordon, Proc. Soc. Photo-Opt. Instrum. Eng. **1860,** 123 (1993).
15. A. Sullivan, H. Hamster, H. C. Kapteyn, S. Gordon, W. White, H. Nathel, R. J. Blair, and R. W. Falcone, Opt. Lett. **16,** 1406 (1991).
16. C. G. Granqvist and O. Hunderi, Phys. Rev. B **16,** 3513 (1977).
17. L. Harris and J. K. Beasley, J. Opt. Soc. Am. **42,** 134 (1952).
18. V. A. Markel, L. S. Muratov, M. I. Stockman, and T. F. George, Phys. Rev. B **43,** 8183 (1991).
19. P. O'Neill and A. Ignatiev, Phys. Rev. B **18,** 6540 (1978).
20. U. Kreibig, A. Althoff, and H. Pressmann, Surf. Sci. **106,** 308 (1981).
21. G. Zaeschmar and A. Nedoluha, J. Opt. Soc. Am. **62,** 348 (1972).
22. G. A. Kyrala, R. D. Fulton, E. K. Wahlin, L. A. Jones, G. T. Schappert, J. A. Cobble, and A. J. Taylor, Appl. Phys. Lett. **60,** 2195 (1992).